

Drozdov, A. Y., Aseev, N., Effenberger, F., Turner, D. L., Saikin, A. A., Shprits, Y. (2019): Storm Time Depletions of Multi-MeV Radiation Belt Electrons Observed at Different Pitch Angles. - Journal of Geophysical Research: Space Physics, 124, 11, 8943-8953.

<https://doi.org/10.1029/2019JA027332>



JGR Space Physics

RESEARCH ARTICLE

10.1029/2019JA027332

Special Section:

Particle Dynamics in the Earth's Radiation Belts

Key Points:

- Up to 49% of the studied storms result in a depletion of multi-MeV electrons, with most depletions at $L^* < 5.2$ are consistent with EMIC waves
- The percentage of storms that result in multi-MeV electron depletions is dependent upon pitch angle
- The number of storm depletions at small pitch angles is higher (increase up to 19%) than the number of depletions at large pitch angles

Supporting Information:

- Supporting Information S1

Correspondence to:

A. Y. Drozdov,
adrozdov@ucla.edu

Citation:

Drozdov, A. Y., Aseev, N., Effenberger, F., Turner, D. L., Saikin, A., & Shprits, Y. (2019). Storm time depletions of multi-MeV radiation belt electrons observed at different pitch angles. *Journal of Geophysical Research: Space Physics*, 124, 8943–8953. <https://doi.org/10.1029/2019JA027332>

Received 23 AUG 2019

Accepted 26 OCT 2019

Accepted article online 07 NOV 2019

Published online 22 NOV 2019

Storm Time Depletions of Multi-MeV Radiation Belt Electrons Observed at Different Pitch Angles

A. Y. Drozdov¹ , N. Aseev^{2,3} , F. Effenberger² , D. L. Turner⁴ , A. Saikin¹ , and Y. Y. Shprits^{1,2,3}

¹Department of Earth, Planetary, and Space Sciences, University of California, Los Angeles, CA, USA, ²GFZ German Research Centre for Geosciences, Potsdam, Germany, ³Institute of Physics and Astronomy, University of Potsdam, Potsdam, Germany, ⁴Space Sciences Department, The Aerospace Corporation, CA, USA

Abstract During geomagnetic storms, the rapid depletion of the high-energy (several MeV) outer radiation belt electrons is the result of loss to the interplanetary medium through the magnetopause, outward radial diffusion, and loss to the atmosphere due to wave-particle interactions. We have performed a statistical study of 110 storms using pitch angle resolved electron flux measurements from the Van Allen Probes mission and found that inside of the radiation belt ($L^* = 3 - 5$) the number of storms that result in depletion of electrons with equatorial pitch angle $\alpha_{eq} = 30^\circ$ is higher than number of storms that result in depletion of electrons with equatorial pitch angle $\alpha_{eq} = 75^\circ$. We conclude that this result is consistent with electron scattering by whistler and electromagnetic ion cyclotron waves. At the outer edge of the radiation belt ($L^* \geq 5.2$) the number of storms that result in depletion is also large (~40–50%), emphasizing the significance of the magnetopause shadowing effect and outward radial transport.

Plain Language Summary Protons and electrons form a radiation environment around Earth that can change drastically during so called *geomagnetic storms*. In this study, we looked at 110 storms to understand how high-energy electrons can disappear due to different phenomena. We found that it is very common to observe a loss of high-energy electrons after storms. More often such a loss happens far away from the Earth as the electrons cross the boundary of the magnetosphere. However, closer to Earth the electrons are lost most likely due to the interaction with *whistler* and *electromagnetic ion cyclotron waves*, which play an important role in the dynamics of the radiation environment.

1. Introduction

Earth's outer radiation belt is populated by electrons (Russell & Thorne, 1970; Van Allen & Frank, 1959), including ones with energies up to several MeV, which are usually referred to as *ultrarelativistic electrons*. During geomagnetic storms, the electron fluxes exhibit irregular variations over several orders of magnitude causing enhancement or depletion of the fluxes at geostationary orbit (Anderson et al., 2015; Kilpua et al., 2015; Kim et al., 2015; O'Brien et al., 2001) and inside of the radiation belts (Fennell et al., 2012; Friedel et al., 2002; Horne et al., 2009; Kataoka & Miyoshi, 2006; Meredith et al., 2011; Yuan & Zong, 2013a; Zhao et al., 2019; Zhao & Li, 2013). Reeves et al. (2003) showed that almost half of the storms result in a depletion or no change in electron fluxes at energies of approximately 1–3 MeV. Turner et al. (2013) obtained similar statistics during the next solar cycle based on a phase space density (PSD) analysis using different satellite measurements.

Launched in 2012, the Van Allen Probes mission (Mauk et al., 2013) provided measurements of the radiation belt electrons in a wide energy range at low geomagnetic latitudes, allowing the detection of nearly the full trapped population (close to 90° equatorial pitch angle). Those measurements revealed that our understanding of the ultrarelativistic electron dynamics is incomplete. One of the first results of the Van Allen Probes multi-MeV electron measurements showed the formation of the unexpected long-lived storage ring (Baker et al., 2013). The formation of such a storage ring was later explained by Shprits et al. (2013) through modeling of this event including Electromagnetic Ion Cyclotron (EMIC) waves. Mann et al. (2016) argued that EMIC waves alone cannot explain the depletion of the electrons at high-pitch angles and they are not required to define the dominant radiation belts morphology. The authors suggested an alternative mechanism of the fast outward radial diffusion due to the interaction with ultralow frequency (ULF) waves. However, Shprits et al. (2018) performed PSD analysis (see Shprits et al., 2017) and confirmed that the

observed depletion of multi-MeV electrons is consistent with localized loss processes by EMIC waves. The observed PSD profiles showed a deepening minimum which is consistent with rapid scattering by EMIC waves. The long-term simulation of multi-MeV electrons also requires additional loss processes (Drozdov et al., 2015) and can be successful if EMIC waves are considered (Drozdov et al., 2017). Although the formation of the storage ring during storm time is a relatively common phenomena (Pinto et al., 2018; Yuan & Zong, 2013b), it is an example of an incomplete understanding of the multi-MeV electron dynamics.

Turner et al. (2015) performed a statistical study of 52 storm time periods (from September 2012 until February 2015), analyzing the response of the outer radiation belt electrons over a broad range of energies using the MagEIS (Blake et al., 2013) instrument on board of the Van Allen Probes. The authors showed that around 36% of the storms resulted in a depletion of the core electron fluxes (≥ 1 MeV) at high L-shells ($L \geq 4$). The storms were selected using the *SYM-H* index threshold of -50 nT, excluding consecutive (within two-day window) events. The authors used omnidirectional electron flux measurements binned over L-shell ($\Delta L = 0.1$) and time ($\Delta t = 6$ hr). To categorize the response of the radiation belt to the storms, they compared maximum prestorm and poststorm flux values at each energy and L-shell. The authors defined the prestorm flux from -84 to -12 hr before the minimum of the *SYM-H* index, and the poststorm flux from $+12$ to $+84$ hr. The event was labeled as depletion if the maximum of the poststorm flux value was lower by a factor of 2 in comparison to the maximum of the prestorm flux value.

Recently, Moya et al. (2017) and Turner et al. (2019) performed similar studies considering electrons of higher energies (up to multi-MeV) and including more storms. Moya et al. (2017) used pitch angle averaged fluxes of the first four years of the Van Allen Probes mission (from September 2012 until June 2016, covering 78 storms) and binned the measurements over L-shell ($\Delta L = 0.1$) and time ($\Delta t = 4$ hr). They compared the maximum flux during 48 hr before and after the storms, excluding the main and most of the recovery phase of the storm. Turner et al. (2019) considered a longer period (from September 2012 until September 2017) and selected 110 storms. The authors used omnidirectional fluxes and followed the same methodology as described in Turner et al. (2015). Moya et al. (2017) and Turner et al. (2019) confirmed the results of previous studies showing the distinctly high probability of MeV and multi-MeV radiation belt electron depletion ($\sim 30\text{--}40\%$) during storms. Turner et al. (2019) reported a feature in the statistical results, where ≥ 1.5 -MeV electrons displayed a stronger tendency for depletion during or/and after storms compared to lower energy electrons, and suggested that this might be the result of losses due to interactions with EMIC waves. However, their analysis was limited to omnidirectional electron fluxes, and did not include an investigation of the electron flux dynamics at different pitch angles. In addition, Boynton et al. (2016, 2017) performed the analysis of the fast electron dropouts using Los Alamos National Laboratory spacecraft at geostationary orbit and Global Positioning System (GPS) satellites at $L \sim 4.2$. Based on 15 years of data the authors found significantly more frequent electron flux dropouts at > 1.5 MeV than at lower energy (0.1–0.7 MeV). The governing factors of multi-MeV electron dropouts were different at geostationary orbit (solar wind dynamic pressure) and at $L \sim 4.2$ (southward interplanetary magnetic field). Moreover, some of the dropouts occurred at $L \sim 4.2$ while no dropouts at geostationary orbit were detected suggesting presence of different mechanisms of electron depletion. Therefore, examination of the electron depletion using an analysis of the pitch angle distribution can help to distinguish between different loss processes, such as outward radial diffusion couple with magnetopause shadowing or wave particle interactions with whistler and EMIC waves (e.g., Mourenas et al., 2016; Xiang et al., 2016, 2017).

Pitch angle distributions (PAD) carry information about the nature of the processes that drive the dynamics of the radiation belts. For example, particle flux depletion due to the magnetopause shadowing effect (Li et al., 1997) causes the decrease of the flux at pitch angles closer to 90° due to drift shell splitting. This effect forms butterfly PADs near the edge of the magnetopause (West et al., 1972, 1973). EMIC waves can cause a rapid depletion of multi-MeV electron fluxes at pitch angles closer to field-aligned directions and lead to a narrowing of PADs (e.g., Drozdov et al., 2017; Li et al., 2007; Shprits et al., 2016; Usanova et al., 2014). As EMIC waves are distinctly efficient at scattering of high-energy electrons close to being field-aligned (e.g., Ni et al., 2015), the narrow PADs are a key signature of the wave-particle interaction of multi-MeV electrons with EMIC waves.

Other physical processes can result in various shapes of PADs, such as pancake, flat top, cigar, cap, and 90° minimum (Zhao et al., 2018). The pancake PAD is commonly observed and it is believed to be a result of

pitch angle scattering due to wave-particle interactions accompanied by a loss to the atmosphere (e.g., Lyons et al., 1972). The flat top PAD can be a characteristic of electron acceleration via interactions with chorus waves (Horne et al., 2003) or a transition between pancake and butterfly PADs. Cap, cigar, and 90° minimum PADs are observed for tens to hundreds of keV electrons and can be the result of wave-particle interactions, stretching of the magnetic field or the drift-shell-splitting effect. Additionally, the variation of the PADs can be a result of adiabatic changes.

Although previous studies discuss the potential effect of the EMIC waves on PAD of multi-MeV electrons (e.g., Usanova et al., 2014; Zhao et al., 2018), understanding of the role of EMIC waves in depletion of the electrons during storms remains incomplete. Over the years, numerous studies have been conducted examining the role that geomagnetic activity plays on the generation of EMIC wave activity (Fraser et al., 2010; Halford et al., 2010, 2015; Keika et al., 2013; Meredith et al., 2014; Saikin, 2018; Saikin et al., 2016; Usanova et al., 2012; Wang et al., 2016). During geomagnetic storms, energetic ring current ions are injected deeper into the inner magnetosphere where they overlap with the cold plasmasphere ion populations, allowing EMIC wave excitation (Cornwall, 1965; Criswell, 1969; Fraser et al., 2010; Jordanova et al., 2001). This concept has been supported using observations from Active Magnetospheric Particle Tracer Explorers/Charge Composition Explorer (AMPTE/CCE; Keika et al., 2013), Akebono (Kasahara et al., 1992), The Combined Release and Radiation Effects Satellite (CRRES; Halford et al., 2010, 2015; Meredith et al., 2014), The Time History of Events and Macroscale Interactions during Substorms (THEMIS) mission (Usanova et al., 2012), and The Van Allen Probes (Saikin, 2018; Saikin et al., 2016), all of which show an increase in EMIC wave occurrence during enhanced geomagnetic activity. Therefore, the presence of EMIC waves during periods of enhanced geomagnetic activity cannot be ignored, especially as it pertains to the scattering of multi-MeV electrons during these storms.

Despite EMIC waves playing a critical role in radiation belt dynamics through the scattering of multi-MeV electrons (Thorne & Kennel, 1971; Lyons et al., 1972; Summers & Throne, 2003; Summers et al., 2007; Jordanova et al., 2008; Zhang et al., 2016, 2017; Qin et al., 2018), large-scale statistical studies on how they impact the PAD of multi-MeV electrons have not been performed. However, the effect of the narrowing of PAD and depletions of multi-MeV electrons flux driven by EMIC waves was only studied during specific storms or short intervals (e.g., Aseev et al., 2017; Bingley et al., 2019; Engebretson et al., 2015; Shprits et al., 2016; Usanova et al., 2014). The statistical studies of the electrons PAD mainly focused on the shape of the distribution and did not consider multi-MeV electron depletions caused by the geomagnetic storms.

In this study, we focus on the depletion of multi-MeV electron fluxes during geomagnetic storms using pitch angle resolved data and statistics of 110 storms. The paper is structured as follows: in section 2 we describe the data set and the methodology used to perform our analysis, in section 3 we discuss the results of our study, and finally we present our conclusions in section 4.

2. Data and Methodology

In this study, we use measurements of the Energetic particle, Composition, and Thermal plasma (ECT) suite (Spence et al., 2013) on board of the Van Allen Probes. The ECT suite includes the Magnetic Electron Ion Spectrometer (MagEIS; Blake et al., 2013) and the Relativistic Electron Proton Telescope (REPT; Baker et al., 2013) instruments. We use electron measurements in the energy range from ~30 keV to ~1.7 MeV from the MagEIS instrument and multi-MeV electron measurements from 1.8 to 6.3 MeV from the REPT instrument. Both MagEIS and REPT observations are pitch angle resolved. We construct 5-min averaged REPT and MagEIS flux data, and then we use the TS05 (Tsyganenko & Sitnov, 2005) magnetic field model to calculate the equatorial value of the pitch angle and generalized L-values or L^* (Roederer, 1970) at every data point (with 5-min interval). Incorporating a magnetic field model which accounts for geomagnetic variations, allows us to reduce the error associated with adiabatic variations.

We follow the methodology described by Turner et al. (2015), Turner et al., 2019 and use the same set of 110 geomagnetic storms between September 2012 and September 2017 as in Turner et al. (2019) to perform the statistical analysis. The storms are identified by the minimum of the *SYM-H* index during the main phase ($SYM-H \leq -50$ nT). Storms that result in several *SYM-H* index minima (e.g., so-called “double-dip” storms) within a 12-hr window are counted as one storm in the data set. We adjust the epoch time to the lowest value of *SYM-H*.

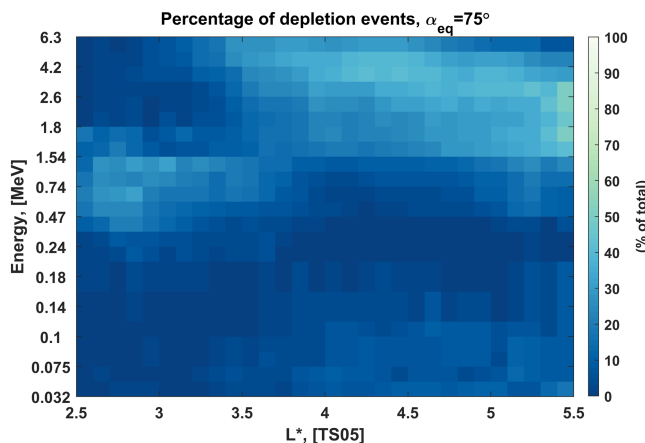


Figure 1. Percentage of events resulting in a depletion of electron fluxes as a function of L^* and electron energy at a 75° equatorial pitch angle.

To explore the electron dynamics statistically, we bin the electron flux in time ($\Delta t = 6$ hr) and L^* ($\Delta L^* = 0.1, L^* \in [2.5; 6.0]$) for each storm. Since the equatorial pitch angle (α_{eq}) values of MagEIS and REPT measurements are different and depend on time, we linearly interpolate the electron flux onto a pitch angle grid $\alpha_{eq} \in [5^\circ; 85^\circ]$ with step size $\Delta\alpha_{eq} = 1^\circ$ before the binning. We use equatorial pitch angles to minimize the effects of adiabatic variations that can affect the pitch angle distribution. This is also a key difference compared with previous similar studies as described in the introduction. Also, in this study, we use the TS05 magnetic field model to calculate L^* (previous studies used L-shell, which is calculated based on the averaged dipole field approximation around the shell).

For every energy, equatorial pitch angle, and L^* , we identify the prestorm and poststorm maximum flux values within 24 hr. We exclude the ± 12 hr around the *storm time* (minimum SYM-H index) to avoid the strong variability of the electron flux during the main phase of the storm. Hence, the prestorm period is defined as -36 to -12 hr before the storm, and the post-storm period as $+12$ to $+36$ hr after the storm. We choose a smaller time window in comparison with previous studies to investigate rapid changes. To validate the sensitivity of the results of this study to the chosen time window, we repeat the analysis using longer time windows (72 hr) and present the results in the supporting information (see details below). An event is labeled as a *depletion event* if the decrease of the poststorm maximum flux value in comparison to the prestorm maximum flux value reaches a factor of 2.

To perform our statistical analysis of the electron radiation belt response, we calculate the percentage of storms that result in electron flux depletion (P_d) due to geomagnetic activity. The percentage P_d is the ratio of the number of storms that result in depletion at the specific energy, equatorial pitch angle, and L^* to the total number of storms.

3. Results and Discussion

Since the orbit of the Van Allen Probes is not perfectly aligned with the equatorial magnetic plane, the measured 90° local pitch angle corresponds to lower equatorial pitch angles. Also, the maximum L^* that the satellites can reach depends on the geomagnetic activity. To ensure that we have enough data points in our statistics we verify the number of valid storms (see Note S1 in the supporting information). The storm is valid if we can determine the prestorm and poststorm maximum flux values for the specific energy, equatorial pitch angle, and L^* . Based on the data validation, we choose our limiting parameters as maximum $\alpha_{eq} = 75^\circ$ and $L^* = 5.5$, and minimum $\alpha_{eq} = 30^\circ$ for the further analysis (see Figure S1 in the supporting information).

Figure 1 shows the calculated percentage P_d for a 75° equatorial pitch angle. This figure is presented in the same format as Figure 2 from Turner et al. (2019) for comparison. Both figures show a similar likelihood of depletion events, even though in this study we use pitch angle resolved fluxes in comparison with the omnidirectional electron fluxes used in the previous studies. The core population of electrons (close to 90° equatorial pitch angle) provides the dominant contribution to the omnidirectional flux. This explains the similarity between the two figures and validates previously obtained results. In addition, the progressive enhancement of the electron flux during storms due to the local acceleration (e.g., Li et al., 2014), inward radial diffusion (e.g., Jaynes et al., 2015), and electron injections (e.g., Turner et al., 2017) can contribute to the weaker probability of the observed low-energy electron depletions (below 1.54 MeV). Also, the lack of electron depletions between 0.10 and 1.54 MeV at $L^* \sim 4$ is consistent with the statistical results of Boynton et al. (2017) obtained for the longer (15 years) period. Overall, Figure 1 shows that 30–40% of the storms result in a depletion of multi-MeV electrons at $\alpha_{eq} = 75^\circ$ in the heart of the outer radiation belt ($L^* \sim 3.5 – 4.5$), which indicates that previous studies reported the depletion of near-equatorial electrons. The large number of depletion events is observed down to $L^* = 3.5$, which is close to the inner edge of the outer electron radiation belts. This effect can be the result of wave-particle interactions with whistler and EMIC waves. Since the scattering of high-energy electrons by EMIC waves results in a narrowing of the

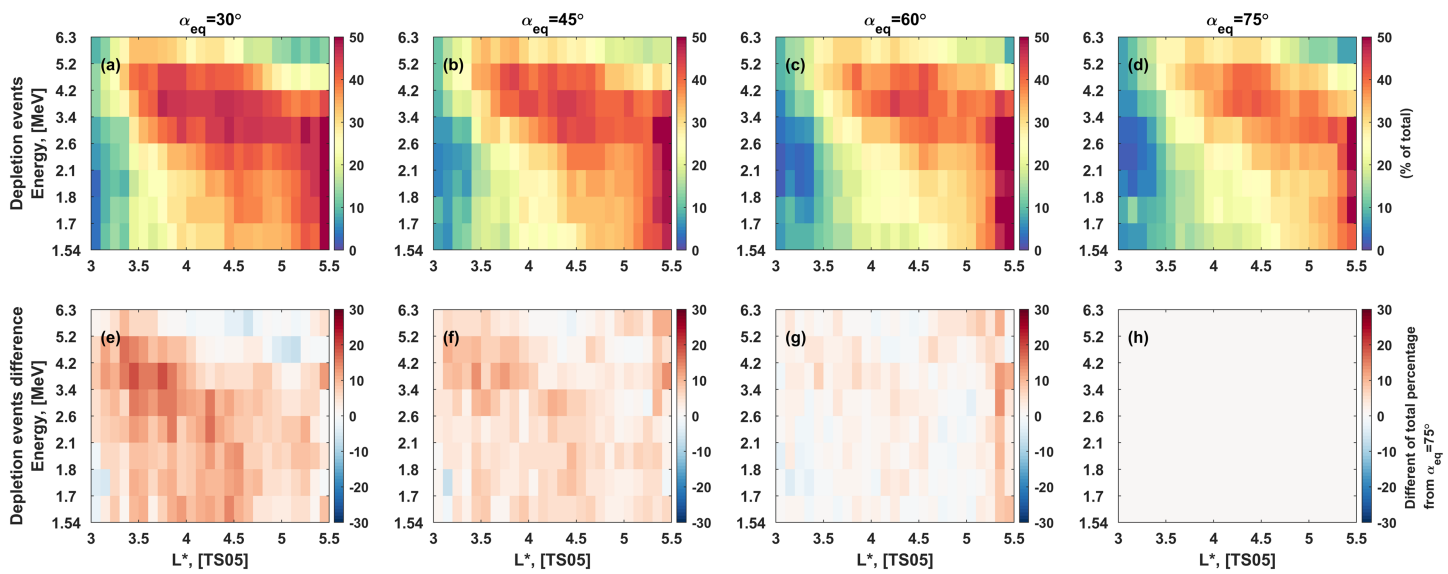


Figure 2. Percentage of events resulting in a depletion of multi-MeV electron fluxes as a function of L^* and electron energy at different equatorial pitch angle (a–d) $\alpha_{eq} = 30^\circ, 45^\circ, 60^\circ, 75^\circ$, respectively. (e–h) The difference of the percentages in (a)–(d) in comparison to (d).

pitch angle distribution, we determine the percentage of storms that result in a depletion at different pitch angles $P_d(\alpha_{eq})$ focusing on multi-MeV energies.

Figure 2 (top row) shows the percentage of depletion events for multi-MeV electrons (≥ 1.54 MeV) at different equatorial pitch angles. The color bar and color scheme of the figure are chosen to enhance the differences between panels. One can see that the percentage P_d of depletion generally increases with decreasing pitch angle. The number of storms that result in a depletion of small pitch angle electrons (e.g., $\alpha_{eq} \sim 30^\circ$) is larger than the same number of more trapped (e.g., $\alpha_{eq} \sim 75^\circ$) electrons. Considering that such a depletion is observed at ultrarelativistic energies on a short time scale (24-hr time window), this indicates a possible scattering by EMIC waves. For a quantitative comparison, Figure 2 (bottom) shows the difference (ΔP_d) of the percentages in comparison to those at $\alpha_{eq} = 75^\circ$, that is,

$$\Delta P_d(\alpha_{eq}) = P_d(\alpha_{eq}) - P_d(\alpha_{eq} = 75^\circ).$$

The positive difference $\Delta P_d(\alpha_{eq} = 30^\circ)$ at L^* between 3 and 5 (see Figure 2e) again indicates the potential effects of EMIC waves. Also, the difference around L^* 3–4 at energies 2.6–5.2 MeV is noticeably larger (up to 19%). This indicates that the electron depletion inside the outer radiation belt far from the magnetopause boundary in the energy range of effective EMIC waves scattering occurs during up to 49% of the storms.

At high L^* ($L^* \geq 5.2$) the percentage P_d between 1.54 and 5.2 MeV is visibly larger (~40–50%) in comparison to lower L^* . This effect can be explained by magnetopause shadowing, which operates at high L^* . The low percentage at higher energies (above 5.2 MeV) in the same L^* region can be explained by the generally low flux level of such high-energy electrons at the outer edge of the radiation belt. The flux level can stay within the background noise indicating no change (the flux level stays within the factor of 2).

We perform several tests to validate our results. We repeat the analysis above for a longer prestorm and post-storm time window of 72 hr (see Figure S2) to ensure that the results are reliable at the selected time window. We discuss the results of this analysis in Note S2. Furthermore, we verify that an increase of the depletion events of multi-MeV electrons with decreasing pitch angle is not a result of adiabatic changes by examining the percentage P_d of the depletion events at lower energies (≤ 1.54 MeV) and different pitch angles (see Figure 3). Changes in the configuration of the magnetic field can lead to the adiabatic change of the PAD. For example, assuming that magnetic field line stretching is occurring, it is expected that electrons of different energies will behave similarly. However, Figure 3 shows that the difference ΔP_d at lower energies is negligibly small, which indicates that the positive difference ΔP_d at multi-MeV energies (Figure 2) is not a result

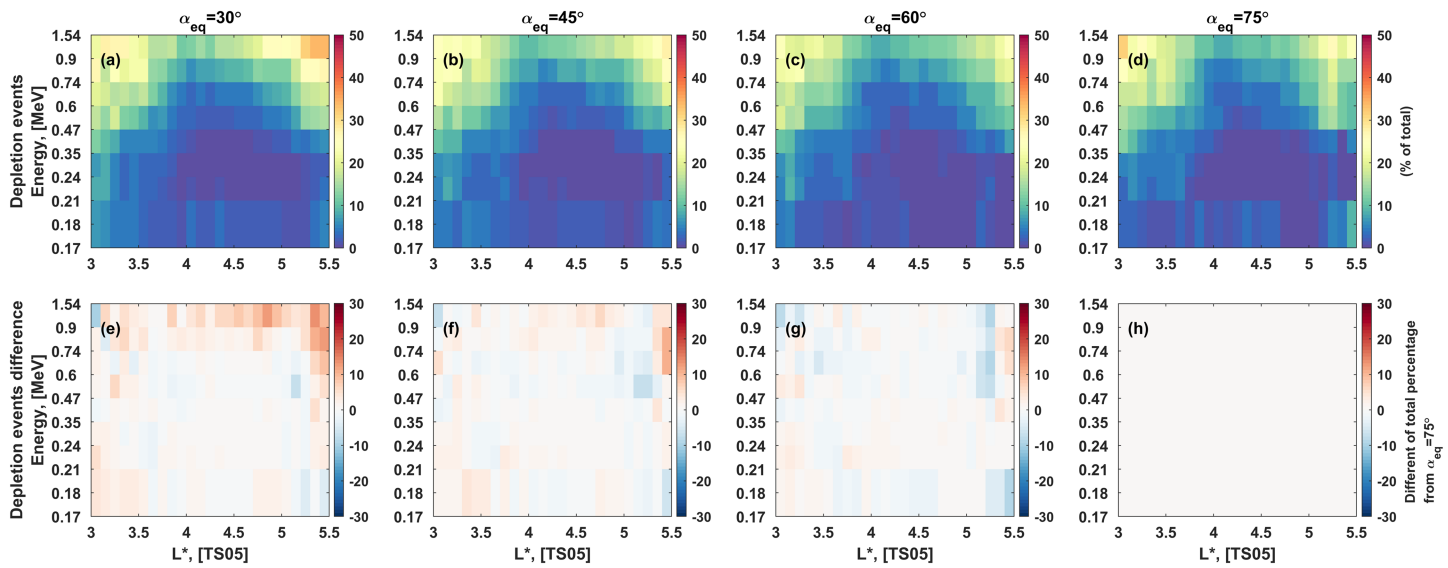


Figure 3. Same as Figure 2 but for energies between 0.17 and 1.54 MeV.

of the adiabatic changes. Finally, we investigate the noticeably large percentage of depletion events at low L^* between 2.5 and 3.5 at energies between 0.47 and 1.54 MeV (see Figure 1). We analyze the sensitivity of the result to the low flux level and conclude that the observed feature is most likely caused by errors related to the background flux level (see Note S3 and Figures S3 and S4).

To analyze the PADs we create two individual lists of the depletion events that occur at high energies of 3.4 and 4.2 MeV at $L^* = 4$ (one list per energy). Forty-six storms result in a depletion at 3.4 MeV and $\alpha_{eq} = 30^\circ$ (first list), and 42 storms result in a depletion at 4.2 MeV and the same equatorial pitch angle (second list). For each list, we calculate prestorm PADs at 36 hr before, and poststorm PADs at 36 hr, and 72 hr after the storm time. Then, we normalize obtained PADs at $\alpha_{eq} = 75^\circ$. From those PADs, we analyze the depletion events with possible change of the PAD that can be a tell-tail signature of EMIC wave activities as discussed above. Figures 4c and 4d show the median of normalized PADs before and after the storm time that result in the depletion of the high-energy electrons at $\alpha_{eq} = 30^\circ$.

The PADs after storms become narrower as energy increases, which can be an indication of EMIC waves scattering. However, a narrowing of the PAD can occur due to the decrease of the magnetic field during the main phase of the storm leading to an adiabatic change. Due to the conservation of the first adiabatic invariant, the decrease of the magnetic field leads to the decrease of the perpendicular component of the

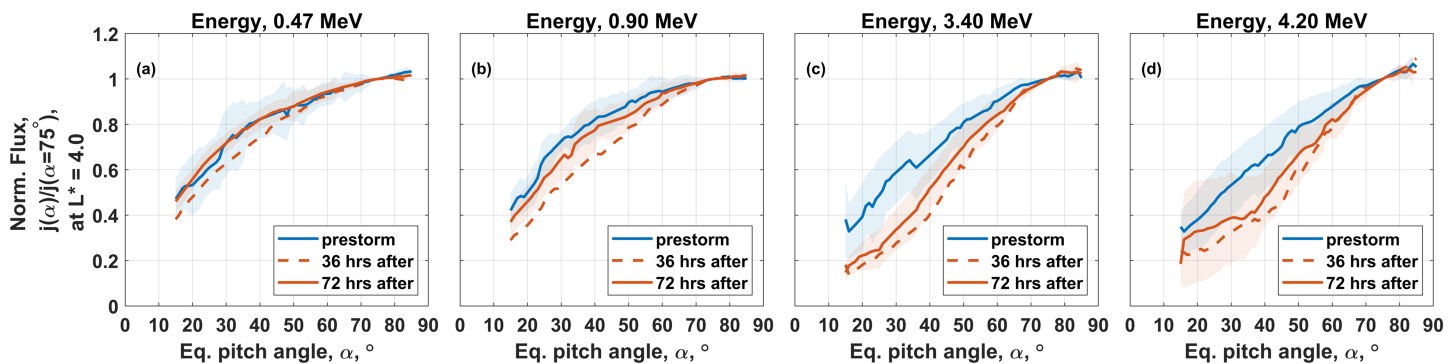


Figure 4. Normalized median PADs 36 hr before (prestorm), 36 hr after, and 72 hr after the storm time that result in a depletion of electrons at $\alpha_{eq} = 30^\circ$ at $L^* = 4$. (a and b) PADs of 0.47- and 0.74-MeV electrons, respectively, during the depletion events at energies of 3.4 and 4.2 MeV. (c and d) PADs of 3.4- and 4.2-MeV electrons, respectively, during the depletion events at the corresponding energy. The colored areas correspond to range of median absolute deviation.

electron's momentum and hence to a flatter PAD. However, as the drift shell expands during the main phase of the storm, the electron bounce trajectories shift to longer field lines. Due to the conservation of the second adiabatic invariant, the parallel component of the electron momentum decreases, leading to a narrowing of the PAD. If the change of the parallel component of the momentum is larger than the change of the perpendicular component, the resulting PAD becomes narrower. Such an adiabatic change should also be observed at lower energies. Note that an exact estimation of the adiabatic changes is difficult because it depends on the steepness of the energy spectrum and radial gradients. However, the adiabatic changes are reversible, and the shape of the PAD can return to its initial state.

To analyze PADs at lower energies (0.47 and 0.74 MeV), we create a third list of depletion events that occur simultaneously at high energies of 3.4 and 4.2 MeV at $L^* = 4.39$. 39 storms result in a depletion at both energies. Figures 4a and 4b show that the normalized PADs of the low-energy electrons also become narrower 36 hr after the storm time; however, the PADs return to the same shape as prestorm PADs after 72 hr after the storm (solid red line). Hence, the effect of adiabatic narrowing of the PAD is almost negligible in comparison with the high-energy electrons (Figures 4c and 4d). This indicates that EMIC wave scattering can play a potentially important role in the formation of a narrow PAD of high-energy electrons, which is supported by the simultaneous lack of significant narrowing at lower energies, excluding an adiabatic variation effect acting at all energies (see also Figure S5).

4. Conclusions

In this study, we have performed a statistical analysis of 110 storms to understand the response of high-energy electrons in the outer radiation belts to geomagnetic storms at different equatorial pitch angles. We found that about 30–40% of the storms result in a depletion of multi-MeV electrons (≥ 1.54 MeV) with an equatorial pitch angle of 75° in the heart of outer radiation belt ($L^* \sim 3.5 - 4.5$). This result is in agreement with findings by Turner et al. (2019) and Moya et al. (2017), who performed a similar analysis using omnidirectional and pitch angle averaged fluxes. Through analyzing the percentage of depletion events at different equatorial pitch angles, we found that more storms result in a depletion of the small pitch angle electrons ($\alpha_{eq} = 30^\circ$) in comparison to the near-equatorial electrons ($\alpha_{eq} = 75^\circ$) inside of the outer radiation belt. Specifically, the likelihood of the depletion events exceeds 40% (reaching 49%) at L^* near 3–4 and energies between 2.6 and 5.2 MeV and $\alpha_{eq} = 30^\circ$. Additionally, we investigated the rapid changes of the electron radiation belts during storms as EMIC waves can provide very fast electron scattering.

There are two possible mechanisms that can cause rapid electron depletion. First, electrons can be rapidly lost due to the magnetopause shadowing effect (e.g., Hudson et al., 2014; Sibeck et al., 1987) coupled with outward radial diffusion (Shprits et al., 2006; Turner et al., 2012). The second mechanism occurs in the heart of the radiation belts ($L^* = 4.5$) and below. Precipitation into the atmosphere can cause a rapid electron flux depletion due to wave-particle interactions (e.g., Green et al., 2004 ; Millan & Thorne, 2007 ; Summers et al., 2007). In the first case, large pitch angle electrons are likely to encounter the magnetopause on the drift orbit forming butterfly pitch angle distribution (e.g., Kim et al., 2008). Our analyses showed that a large fraction of storms result in a depletion of electrons at high L^* (≥ 5.2) at all considered pitch angles ($\alpha_{eq} = 30^\circ - 75^\circ$), which can be explained by the magnetopause shadowing effect and outward radial diffusion. However, at lower L^* (< 5.2), the number of storms that result in a depletion of multi-MeV electrons increases with decreasing equatorial pitch angle, which is unlikely to be explained by outward radial diffusion or the magnetopause shadowing effect alone. However, a fast outward radial diffusion can potentially produce rapid electron depletion down to $L^* = 4$, but it requires large-amplitude ULF waves (Ukhorskiy et al., 2009). During such storms chorus waves can accelerate previously depleted electrons at large pitch angles ($\alpha_{eq} \gtrsim 50^\circ$) forming observed narrower poststorm PAD in comparison to the prestorm PAD (Horne et al., 2005; Li et al., 2014; Thorne et al., 2013). Although, this scenario implies the simultaneous electron depletion over wide L^* range and does not explain the observed larger number of storms that results in a depletion at $L^* < 5.2$. In addition, chorus wave acceleration competes with the second loss mechanism (wave-particle interaction induced precipitation to the atmosphere). For example, the competing loss and source mechanisms were observed during the storm that occurred from 30 September to 3 October 2012. During this storm, chorus waves provided local acceleration of the electrons while EMIC waves were the dominant wave-particle interaction resulting in an overall depletion of the high-energy electrons with first adiabatic

invariant $\mu \gtrsim 1200$ MeV/G (Turner et al., 2014). We conclude that the observed difference in the percentage of the storms that result in a depletion at different pitch angles is consistent with EMIC wave activity.

EMIC waves can provide a rapid scattering of relativistic electrons (>1 MeV) and are not sufficient for significant depletion of the lower energy electrons (e.g., Lyons & Thorne, 1972; Meredith et al., 2013; Thorne & Kennel, 1971). Recent studies show that only multi-MeV electrons can be affected by EMIC waves (Drozdov et al., 2017; Mourenas et al., 2016; Pinto et al., 2019; Shprits et al., 2013; Shprits et al., 2016; Shprits et al., 2018; Usanova et al., 2014; Yuan et al., 2018). Our results show that the number of depletion events of electrons below 1.54 MeV is negligible in comparison to multi-MeV electrons as the population of multi-MeV electrons requires an additional loss mechanism (e.g., Drozdov et al., 2015; Shprits et al., 2013; Shprits et al., 2016). In addition, EMIC waves affect electrons with small pitch angles and do not resonate with the near-equatorial electrons (e.g., Albert, 2003). As a result, more storms result in a depletion of multi-MeV electrons at $\alpha_{eq} = 30^\circ$ in comparison to $\alpha_{eq} = 75^\circ$ at $L^* < 5.2$. Also, the poststorm pitch angle distributions of the multi-MeV electrons become more narrow, representing a distinct signature of EMIC wave activity (e.g., Shprits et al., 2016; Usanova et al., 2014), while the pitch angle distributions at lower energies (<1.54 MeV) do not show significant changes. In summary, almost half of the observed storms result in a depletion of multi-MeV electrons according to the chosen criteria. However, due to the described competing mechanisms, comprehensive modeling and additional data analysis are required to determine the appropriate cause of the depletion events. The systematic analysis of electron PSD profiles, pitch angle distributions, and the search for PSD minima will help to distinguish between the different mechanisms that drive radiation belts dynamics and will be the subject of future research.

Acknowledgments

The authors are grateful to the RBSP-ECT team for the provision of Van Allen Probes data (<http://rbsp-ect.lanl.gov/>). This research is supported by NASA awards 80NSSC18K0663 and NNX16AF91G. The authors thank Dominika Boneberg for the help with the manuscript preparation.

References

- Albert, J. M. (2003). Evaluation of quasi-linear diffusion coefficients for EMIC waves in a multispecies plasma. *Journal of Geophysical Research* 108(A6), 1249. Retrieved from <https://onlinelibrary.wiley.com/doi/abs/10.1029/2002JA009792>
- Anderson, B. R., Millan, R. M., Reeves, G. D., & Friedel, R. H. W. (2015). Acceleration and loss of relativistic electrons during small geomagnetic storms. *Geophysical Research Letters* 42, 10,113–10,119. <https://doi.org/10.1002/2015GL066376>
- Aseev, N. A., Shprits, Y. Y., Drozdov, A. Y., Kellerman, A. C., Usanova, M. E., Wang, D., & Zhelavskaya, I. S. (2017). Signatures of Ultrarelativistic Electron Loss in the Heart of the Outer Radiation Belt Measured by Van Allen Probes. *Journal of Geophysical Research: Space Physics* 122, 2017JA024485, 10,102–10,111. <https://doi.org/10.1002/2017JA024485>
- Baker, D. N., Kanekal, S. G., Hoxie, V. C., Batiste, S., Bolton, M., Li, X., et al. (2013). The Relativistic Electron-Proton Telescope (REPT) Instrument on Board the Radiation Belt Storm Probes (RBSP) Spacecraft: Characterization of Earth's Radiation Belt High-Energy Particle Populations. *Space Science Reviews* 179(1–4), 337–381. <https://doi.org/10.1007/s11214-012-9950-9>
- Bingley, L., Angelopoulos, V., Sibeck, D., Zhang, X., & Halford, A. (2019). The Evolution of a Pitch-Angle 'Bite-Out' Scattering Signature Caused by EMIC Wave Activity: A Case Study. *Journal of Geophysical Research: Space Physics* 124(7), 5042–5055. <https://doi.org/10.1029/2018JA026292>
- Blake, J. B., Carranza, P. A., Claudepierre, S. G., Clemons, J. H., Crain, W. R. Jr., Dotan, Y., et al. (2013). The Magnetic Electron Ion Spectrometer (MagEIS) Instruments Aboard the Radiation Belt Storm Probes (RBSP) Spacecraft. *Space Science Reviews* 179(1–4), 383–421. <https://doi.org/10.1007/s11214-013-9991-8>
- Boynton, R. J., Mourenas, D., & Balikhin, M. A. (2016). Electron flux dropouts at Geostationary Earth Orbit: Occurrences, magnitudes, and main driving factors. *Journal of Geophysical Research: Space Physics* 121, 8448–8461. <https://doi.org/10.1002/2016JA022916>
- Boynton, R. J., Mourenas, D., & Balikhin, M. A. (2017). Electron Flux Dropouts at $L \sim 4.2$ From Global Positioning System Satellites: Occurrences, Magnitudes, and Main Driving Factors: DROPOUTS ON GPS ORBIT. *Journal of Geophysical Research: Space Physics* 122, 11,428–11,441. <https://doi.org/10.1002/2017JA024523>
- Cornwall, J. M. (1965). Cyclotron instabilities and electromagnetic emission in the ultra low frequency and very low frequency ranges. *Journal of Geophysical Research* 70(1), 61–69. <https://doi.org/10.1029/JZ070i001p00061>
- Criswell, D. R. (1969). Pc 1 micropulsation activity and magnetospheric amplification of 0.2- to 5.0-Hz hydromagnetic waves. *Journal of Geophysical Research* 74(1), 205–224. <https://doi.org/10.1029/JA074i001p00205>
- Drozdov, A. Y., Shprits, Y. Y., Orlova, K. G., Kellerman, A. C., Subbotin, D. A., Baker, D. N., et al. (2015). Energetic, relativistic, and ultrarelativistic electrons: Comparison of long-term VERB code simulations with Van Allen Probes measurements. *Journal of Geophysical Research: Space Physics* 120, 3574–3587. <https://doi.org/10.1002/2014JA020637>
- Drozdov, A. Y., Shprits, Y. Y., Usanova, M. E., Aseev, N. A., Kellerman, A. C., & Zhu, H. (2017). EMIC wave parameterization in the long-term VERB code simulation. *Journal of Geophysical Research: Space Physics* 122, 2017JA024389, 8488–2017JA028501. <https://doi.org/10.1002/2017JA024389>
- Engebretson, M. J., Posch, J. L., Wygant, J. R., Kletzing, C. A., Lessard, M. R., Huang, C. L., et al. (2015). Van Allen probes, NOAA, GOES, and ground observations of an intense EMIC wave event extending over 12 h in magnetic local time: EMIC WAVES AND THE RADIATION BELTS. *Journal of Geophysical Research: Space Physics* 120, 5465–5488. <https://doi.org/10.1002/2015JA021227>
- Fennell, J. F., Kanekal, S., & Roeder, J. L. (2012). Storm Responses of Radiation Belts During Solar Cycle 23: HEO Satellite Observations: Summers/Dynamics of the Earth's Radiation Belts and Inner Magnetosphere. In D. Summers, I. R. Mann, D. N. Baker, & M. Schulz (Eds.), *Dynamics of the Earth's Radiation Belts and Inner Magnetosphere*, vol. 155, (pp. 371–384). Washington, D. C.: American Geophysical Union.
- Fraser, B. J., Grew, R. S., Morley, S. K., Green, J. C., Singer, H. J., Loto'anui, T. M., & Thomsen, M. F. (2010). Storm time observations of electromagnetic ion cyclotron waves at geosynchronous orbit: GOES results: EMIC WAVES AND STORMS, GOES RESULTS. *Journal of Geophysical Research* 115(A5). <https://doi.org/10.1029/2009JA014516>

- Friedel, R. H. W., Reeves, G. D., & Obara, T. (2002). Relativistic electron dynamics in the inner magnetosphere — a review. *Journal of Atmospheric and Solar-Terrestrial Physics* 64(2), 265–282. [https://doi.org/10.1016/S1364-6826\(01\)00088-8](https://doi.org/10.1016/S1364-6826(01)00088-8)
- Green, J. C., Onsager, T. G., O'Brien, T. P., & Baker, D. N. (2004). Testing loss mechanisms capable of rapidly depleting relativistic electron flux in the Earth's outer radiation belt. *Journal of Geophysical Research* 109(A12), A12211. <https://doi.org/10.1029/2004JA010579>
- Halford, A. J., Fraser, B. J., & Morley, S. K. (2010). EMIC wave activity during geomagnetic storm and nonstorm periods: CRRES results. *Journal of Geophysical Research* 115, A12248. <https://doi.org/10.1029/2010JA015716>
- Halford, A. J., Fraser, B. J., & Morley, S. K. (2015). EMIC waves and plasmaspheric and plume density: CRRES results. *Journal of Geophysical Research: Space Physics* 120, 1974–1992. <https://doi.org/10.1002/2014JA020338>
- Horne, R. B., Lam, M. M., & Green, J. C. (2009). Energetic electron precipitation from the outer radiation belt during geomagnetic storms. *Geophysical Research Letters* 36, 1249. <https://doi.org/10.1029/2009GL040236>
- Horne, R. B., Meredith, N. P., Thorne, R. M., Heynderickx, D., Iles, R. H. A., & Anderson, R. R. (2003). Evolution of energetic electron pitch angle distributions during storm time electron acceleration to megaelectronvolt energies. *Journal of Geophysical Research* 108(A1), SMP 11–1–SMP 11–13. 1016. <https://doi.org/10.1029/2001JA009165>
- Horne, R. B., Thorne, R. M., Glauert, S. A., Albert, J. M., Meredith, N. P., & Anderson, R. R. (2005). Timescale for radiation belt electron acceleration by whistler mode chorus waves. *Journal of Geophysical Research* 110(A3), 2429. <https://doi.org/10.1029/2004JA010811>
- Hudson, M. K., Baker, D. N., Goldstein, J., Kress, B. T., Paral, J., Toffoletto, F. R., & Wiltberger, M. (2014). Simulated magnetopause losses and Van Allen Probe flux dropouts. *Geophysical Research Letters* 41, 1113–1118. <https://doi.org/10.1002/2014GL059222>
- Jaynes, A. N., Baker, D. N., Singer, H. J., Rodriguez, J. V., Loto'aniu, T. M., Ali, A. F., et al. (2015). Source and seed populations for relativistic electrons: Their roles in radiation belt changes. *Journal of Geophysical Research: Space Physics* 120, 7240–7254. <https://doi.org/10.1002/2015JA021234>
- Jordanova, V. K., Albert, J., & Miyoshi, Y. (2008). Relativistic electron precipitation by EMIC waves from self-consistent global simulations. *Journal of Geophysical Research* 113, A00A10–A00A21. <https://doi.org/10.1029/2008JA013239>
- Jordanova, V. K., Farrugia, C. J., Thorne, R. M., Khazanov, G. V., Reeves, G. D., & Thomsen, M. F. (2001). Modeling ring current proton precipitation by electromagnetic ion cyclotron waves during the May 14–16, 1997, storm. *Journal of Geophysical Research* 106(A1), 7–22. <https://doi.org/10.1029/2000JA002008>
- Kasahara, Y., Sawada, A., Yamamoto, M., Kimura, I., Kokubun, S., & Hayashi, K. (1992). Ion cyclotron emissions observed by the satellite Akebono in the vicinity of the magnetic equator. *Radio Science* 27(2), 347–362. <https://doi.org/10.1029/91RS01872>
- Kataoka, R., & Miyoshi, Y. (2006). Flux enhancement of radiation belt electrons during geomagnetic storms driven by coronal mass ejections and corotating interaction regions: RADIATION BELT DURING CME/CIR STORMS. *Space Weather* 4, S09004. <https://doi.org/10.1029/2005SW000211>
- Keika, K., Takahashi, K., Ukhorskiy, A. Y., & Miyoshi, Y. (2013). Global characteristics of electromagnetic ion cyclotron waves: Occurrence rate and its storm dependence: GLOBAL CHARACTERISTICS OF EMIC WAVES. *Journal of Geophysical Research: Space Physics* 118, 4135–4150. <https://doi.org/10.1002/jgra.50385>
- Kilpua, E. K. J., Hietala, D. L., Turner, H. E. J., Koskinen, T. I., Pulkkinen, J. V., Rodriguez, et al. (2015). Unraveling the drivers of the storm time radiation belt response. *Geophysical Research Letters* 42, <https://doi.org/10.1002/2015GL063542>, 3076, 3084.
- Kim, H.-J., Lyons, L., Pinto, V., Wang, C.-P., & Kim, K.-C. (2015). Revisit of relationship between geosynchronous relativistic electron enhancements and magnetic storms: STORMS AND ELECTRON ENHANCEMENTS AT GEO. *Geophysical Research Letters* 42, 6155–6161. <https://doi.org/10.1002/2015GL065192>
- Kim, K. C., Lee, D.-Y., Kim, H.-J., Lyons, L. R., Lee, E. S., Öztürk, M. K., & Choi, C. R. (2008). Numerical calculations of relativistic electron drift loss effect. *Journal of Geophysical Research* 113(A9). <https://doi.org/10.1029/2007JA013011>
- Li, W., Shprits, Y. Y., & Thorne, R. M. (2007). Dynamic evolution of energetic outer zone electrons due to wave-particle interactions during storms. *Journal of Geophysical Research* 112, A10220. <https://doi.org/10.1029/2007JA012368>
- Li, W., Thorne, R. M., Ma, Q., Ni, B., Bortnik, J., Baker, D. N., et al. (2014). Radiation belt electron acceleration by chorus waves during the 17 March 2013 storm. *Journal of Geophysical Research: Space Physics* 119, 4681–4693. <https://doi.org/10.1002/2014JA019945>
- Li, X., Baker, D. N., Temerin, M., Cayton, T. E., Reeves, E. G. D., Christensen, R. A., et al. (1997). Multisatellite observations of the outer zone electron variation during the November 3–4, 1993, magnetic storm. *Journal of Geophysical Research* 102(A7), 14123–14140. <https://doi.org/10.1029/97JA01101>
- Lyons, L. R., & Thorne, R. M. (1972). Parasitic pitch angle diffusion of radiation belt particles by ion cyclotron waves. *Journal of Geophysical Research* 77(28), 5608–5616. <https://doi.org/10.1029/JA077i028p05608>
- Lyons, L. R., Thorne, R. M., & Kennel, C. F. (1972). Pitch-angle diffusion of radiation belt electrons within the plasmasphere. *Journal of Geophysical Research* 77(19), 3455–3474. <https://doi.org/10.1029/JA077i019p03455>
- Mann, I. R., Ozeke, L. G., Murphy, K. R., Claudepierre, S. G., Turner, D. L., Baker, D. N., et al. (2016). Explaining the dynamics of the ultra-relativistic third Van Allen radiation belt. *Nature Physics* 12(10), 978–983. <https://doi.org/10.1038/nphys3799>
- Mauk, B. H., Fox, N. J., Kanekal, S. G., Kessel, R. L., Sibeck, D. G., & Ukhorskiy, A. (2013). Science Objectives and Rationale for the Radiation Belt Storm Probes Mission. *Space Science Reviews* 179(1–4), 3–27. <https://doi.org/10.1007/s11214-012-9908-y>
- Meredith, N. P., Horne, R. B., Bortnik, J., Thorne, R. M., Chen, L., Li, W., & Sicard-Piet, A. (2013). Global statistical evidence for chorus as the embryonic source of plasmaspheric hiss: SOURCE OF PLASMASPERHERIC HISS. *Geophysical Research Letters* 40, 2891–2896. <https://doi.org/10.1002/grl.50593>
- Meredith, N. P., Horne, R. B., Kersten, T., Fraser, B. J., & Grew, R. S. (2014). Global morphology and spectral properties of EMIC waves derived from CRRES observations. *Journal of Geophysical Research: Space Physics* 119, 5328–5342. <https://doi.org/10.1002/2014JA020064>
- Meredith, N. P., Horne, R. B., Lam, M. M., Denton, M. H., Borovsky, J. E., & Green, J. C. (2011). Energetic electron precipitation during high-speed solar wind stream driven storms. *Journal of Geophysical Research* 116(A5), 409. <https://doi.org/10.1029/2010JA016293>
- Millan, R. M., and R. M. Thorne (2007). Review of radiation belt relativistic electron losses, *Journal of Geophysical Research* 69, 362–377, doi:<https://doi.org/10.1016/j.jastp.2006.06.019>.
- Mourenas, D., Artemyev, A. V., Ma, Q., Agapitov, O. V., & Li, W. (2016). Fast dropouts of multi-MeV electrons due to combined effects of EMIC and whistler mode waves. *Geophysical Research Letters* 43. <https://doi.org/10.1002/2016GL068921>, 4155, 4163
- Moya, P. S., Pinto, V. A., Sibeck, D. G., Kanekal, S. G., & Baker, D. N. (2017). On the Effect of Geomagnetic Storms on Relativistic Electrons in the Outer Radiation Belt: Van Allen Probes Observations: EFFECT OF STORMS ON THE RADIATION BELTS. *Journal of Geophysical Research: Space Physics* 122, 11,100–11,108. <https://doi.org/10.1002/2017JA024735>

- Ni, B., Cao, X., Zou, Z., Zhou, C., Gu, X., Bortnik, J., et al. (2015). Resonant scattering of outer zone relativistic electrons by multiband EMIC waves and resultant electron loss time scales: ELECTRON SCATTERING BY EMIC WAVES. *Journal of Geophysical Research: Space Physics* 120, 7357–7373. <https://doi.org/10.1002/2015JA021466>
- O'Brien, T. P., McPherron, R. L., Sornette, D., Reeves, G. D., Friedel, R., & Singer, H. J. (2001). Which magnetic storms produce relativistic electrons at geosynchronous orbit? *Journal of Geophysical Research* 106(A8), 15533–15544. <https://doi.org/10.1029/2001JA000052>
- Pinto, V. A., Bortnik, J., Moya, P. S., Lyons, L. R., Sibeck, D. G., Kanekal, S. G., et al. (2018). Characteristics, Occurrence, and Decay Rates of Remnant Belts Associated With Three-Belt Events in the Earth's Radiation Belts. *Geophysical Research Letters* 45(22), 12,099–12,107. <https://doi.org/10.1029/2018GL080274>
- Pinto, V. A., Mourenas, D., Bortnik, J., Zhang, X.-J., Artemyev, A. V., Moya, P. S., & Lyons, L. R. (2019). Decay of Ultrarelativistic Remnant Belt Electrons Through Scattering by Plasmaspheric Hiss. *Journal of Geophysical Research: Space Physics* 124(7), 5222–5233. <https://doi.org/10.1029/2019JA026509>
- Qin, M., Hudson, M., Millan, R., Woodger, L., & Shekhar, S. (2018). Statistical Investigation of the Efficiency of EMIC Waves in Precipitating Relativistic Electrons. *Journal of Geophysical Research: Space Physics* 123(8), 6223–6230. <https://doi.org/10.1029/2018JA025419>
- Reeves, G. D., McAdams, K. L., Friedel, R. H. W., & O'Brien, T. P. (2003). Acceleration and loss of relativistic electrons during geomagnetic storms. *Geophysical Research Letters* 30(10). 1529. <https://doi.org/10.1029/2002GL016513>
- Roederer, J. G. (1970). *Dynamics of Geomagnetically Trapped Radiation*. Berlin, Heidelberg: Springer. <https://doi.org/10.1007/978-3-642-49300-3>
- Russell, C. T., & Thorne, R. M. (1970). On the Structure of the Inner Magnetosphere. In *Cosmic Electrodynamics*, (Vol. 1, pp. 67–89). Dordrecht-Holland: D. Reidel Publishing Company.
- Saikin, A. A. (2018). The spatial distributions, wave properties, and generation mechanisms of inner magnetosphere EMIC waves. *Doctoral Dissertations*. East Eisenhower Parkway Ann Arbor, Michigan: ProQuest:ProQuest LLC.
- Saikin, A. A., Zhang, J.-C., Smith, C. W., Spence, H. E., Torbert, R. B., & Kletzing, C. A. (2016). The dependence on geomagnetic conditions and solar wind dynamic pressure of the spatial distributions of EMIC waves observed by the Van Allen Probes: RBSP EMIC WAVES. *Journal of Geophysical Research: Space Physics* 121, 4362–4377. <https://doi.org/10.1002/2016JA022523>
- Shprits, Y. Y., Drozdov, A. Y., Spasovic, M., Kellerman, A. C., Usanova, M. E., Engebretson, M. J., et al. (2016). Wave-induced loss of ultra-relativistic electrons in the Van Allen radiation belts. *Nature Communications* 7, 12883. <https://doi.org/10.1038/ncomms12883>, 1, 7
- Shprits, Y. Y., Horne, R. B., Kellerman, A. C., & Drozdov, A. Y. (2018). The dynamics of Van Allen belts revisited. *Nature Physics* 14(2), 102–103. <https://doi.org/10.1038/nphys4350>
- Shprits, Y. Y., Kellerman, A., Aseev, N., Drozdov, A. Y., & Michaelis, I. (2017). Multi-MeV electron loss in the heart of the radiation belts. *Geophysical Research Letters*, 44, 1204–1209. <https://doi.org/10.1002/2016gl072258>
- Shprits, Y. Y., Subbotin, D., Drozdov, A., Usanova, M. E., Kellerman, A., Orlova, K., et al. (2013). Unusual stable trapping of the ultrarelativistic electrons in the Van Allen radiation belts. *Nature Physics* 9(11), 699–703. <https://doi.org/10.1038/nphys2760>
- Shprits, Y. Y., Thorne, R. M., Friedel, R., Reeves, G. D., Fennell, J., Baker, D. N., & Kanekal, S. G. (2006). Outward radial diffusion driven by losses at magnetopause. *Journal of Geophysical Research* 111, A11214. <https://doi.org/10.1029/2006JA011657>
- Sibeck, D. G., McEntire, R. W., Lui, A. T. Y., Lopez, R. E., & Krimigis, S. M. (1987). Magnetic field drift shell splitting: Cause of unusual dayside particle pitch angle distributions during storms and substorms. *Journal of Geophysical Research* 92(A12), 13485. <https://doi.org/10.1029/JA092iA12p13485>
- Spence, H. E., Reeves, G. D., Baker, D. N., Blake, J. B., Bolton, M., Bourdarie, S., et al. (2013). Science Goals and Overview of the Radiation Belt Storm Probes (RBSP) Energetic Particle, Composition, and Thermal Plasma (ECT) Suite on NASA's Van Allen Probes Mission. *Space Science Reviews* 179(1–4), 311–336. <https://doi.org/10.1007/s11214-013-0007-5>
- Summers, D., Ni, B., & Meredith, N. P. (2007). Timescales for radiation belt electron acceleration and loss due to resonant wave-particle interactions: 2. Evaluation for VLF chorus, ELF hiss, and electromagnetic ion cyclotron waves. *Journal of Geophysical Research* 112(A4), 1–21. <https://doi.org/10.1029/2006JA011993>
- Summers, D., & Throne, R. M. (2003). Relativistic electron pitch-angle scattering by electromagnetic ion cyclotron waves during geomagnetic storms. *Journal of Geophysical Research* 108(A4), 1–12. <https://doi.org/10.1029/2002JA009489>
- Thorne, R. M., & Kennel, C. F. (1971). Relativistic electron precipitation during magnetic storm main phase. *Journal of Geophysical Research* 76(19), 4446–4453. <https://doi.org/10.1029/JA076i019p04446>
- Thorne, R. M., Li, W., Ni, B., Ma, Q., Bortnik, J., Chen, L., et al. (2013). Rapid local acceleration of relativistic radiation-belt electrons by magnetospheric chorus. *Nature* 504(7480), 411–414. <https://doi.org/10.1038/nature12889>
- Tsyganenko, N. A., & Sitnov, M. I. (2005). Modeling the dynamics of the inner magnetosphere during strong geomagnetic storms. *Journal of Geophysical Research* 110(A3), 7737. <https://doi.org/10.1029/2004JA010798>
- Turner, D. L., Angelopoulos, V., Li, W., Hartinger, M. D., Usanova, M., Mann, I. R., et al. (2013). On the storm-time evolution of relativistic electron phase space density in Earth's outer radiation belt. *Journal of Geophysical Research: Space Physics* 118, 2196–2212. <https://doi.org/10.1002/jgra.50151>
- Turner, D. L., Angelopoulos, V., Li, W., Bortnik, J., Ni, B., Ma, Q., et al. (2014). Competing source and loss mechanisms due to wave-particle interactions in Earth's outer radiation belt during the 30 September to 3 October 2012 geomagnetic storm. *Journal of Geophysical Research: Space Physics*, 119, 1960–1979. <https://doi.org/10.1002/2014ja019770>
- Turner, D. L., Kilpua, E. K. J., Hietala, H., Claudepierre, S. G., O'Brien, T. P., Fennell, J. F., et al. (2019). The response of Earth's electron radiation belts to geomagnetic storms: Statistics from the Van Allen Probes era including effects from different storm drivers. *Journal of Geophysical Research: Space Physics* 124(2), 1013–1034. <https://doi.org/10.1029/2018JA026066>
- Turner, D. L., O'Brien, T. P., Fennell, J. F., Claudepierre, S. G., Blake, J. B., Jaynes, A. N., et al. (2017). Investigating the source of near-relativistic and relativistic electrons in Earth's inner radiation belt. *Journal of Geophysical Research: Space Physics* 122, 695–710. <https://doi.org/10.1002/2016JA023600>
- Turner, D. L., O'Brien, T. P., Fennell, J. F., Claudepierre, S. G., Blake, J. B., Kilpua, E., & Hietala, H. (2015). The effects of geomagnetic storms on electrons in Earth's radiation belts. *Geophysical Research Letters* 42, 2015GL064747, 9176–2015GL069184. <https://doi.org/10.1002/2015GL064747>
- Turner, D. L., Shprits, Y., Hartinger, M., & Angelopoulos, V. (2012). Explaining sudden losses of outer radiation belt electrons during geomagnetic storms. *Nature Physics* 8(3), 208–212. <https://doi.org/10.1038/nphys2185>

- Ukhorskiy, A. Y., Sitnov, M. I., Takahashi, K., & Anderson, B. J. (2009). Radial transport of radiation belt electrons due to stormtime Pc5 waves. *Annals of Geophysics* 27(5), 2173–2181. <https://doi.org/10.5194/angeo-27-2173-2009>
- Usanova, M. E., Drozdov, A., Orlova, K., Mann, I. R., Shprits, Y., Robertson, M. T., et al. (2014). Effect of EMIC waves on relativistic and ultrarelativistic electron populations: Ground-based and Van Allen Probes observations. *Geophysical Research Letters* 41, 1375–1381. <https://doi.org/10.1002/2013GL059024>
- Usanova, M. E., Mann, I. R., Bortnik, J., Shao, L., & Angelopoulos, V. (2012). THEMIS observations of electromagnetic ion cyclotron wave occurrence: Dependence on AE, SYMH, and solar wind dynamic pressure. *Journal of Geophysical Research* 117(A10), 1–13. <https://doi.org/10.1029/2012JA018049>
- Van Allen, J. A., & Frank, L. A. (1959). Radiation Around the Earth to a Radial Distance of 107,400 km. *Nature* 183(4659), 430–434. <https://doi.org/10.1038/183430a0>
- Wang, D., Yuan, Z., Yu, X., Huang, S., Deng, X., Zhou, M., & Li, H. (2016). Geomagnetic storms and EMIC waves: Van Allen Probe observations. *Journal of Geophysical Research: Space Physics* 121, 6444–6457. <https://doi.org/10.1002/2015JA022318>
- West, H. I. Jr., Buck, R. M., & Walton, J. R. (1972). Shadowing of Electron Azimuthal-Drift Motions near the Noon Magnetopause. *Nature Physical Science* 240(97), 6–7. <https://doi.org/10.1038/physci240006a0>
- West, H. I. Jr., Buck, R. M., & Walton, J. R. (1973). Electron pitch angle distributions throughout the magnetosphere as observed on Ogo 5. *Journal of Geophysical Research* 78(7), 1064–1081. <https://doi.org/10.1029/JA078i007p01064>
- Xiang, Z., Ni, B., Zhou, C., Zou, Z., Gu, X., Zhao, Z., et al. (2016). Multi-satellite simultaneous observations of magnetopause and atmospheric losses of radiation belt electrons during an intense solar wind dynamic pressure pulse. *Annals of Geophysics* 34(5), 493–509. <https://doi.org/10.5194/angeo-34-493-2016>
- Xiang, Z., Tu, W., Li, X., Ni, B., Morley, S. K., & Baker, D. N. (2017). Understanding the Mechanisms of Radiation Belt Dropouts Observed by Van Allen Probes. *Journal of Geophysical Research: Space Physics* 122, 9858–9879. <https://doi.org/10.1002/2017JA024487>
- Yuan, C., & Zong, Q. (2013a). Relativistic electron fluxes dropout in the outer radiation belt under different solar wind conditions. *Journal of Geophysical Research: Space Physics* 118, 7545–7556. <https://doi.org/10.1002/2013JA019066>
- Yuan, C., & Zong, Q. (2013b). The double-belt outer radiation belt during CME- and CIR-driven geomagnetic storms. *Journal of Geophysical Research: Space Physics* 118, 6291–6301. <https://doi.org/10.1002/jgra.50564>
- Yuan, Z., Liu, K., Yu, X., Yao, F., Huang, S., Wang, D., & Ouyang, Z. (2018). Precipitation of Radiation Belt Electrons by EMIC Waves With Conjugated Observations of NOAA and Van Allen Satellites. *Geophysical Research Letters* 45(23), A07209. <https://doi.org/10.1029/2018GL080481>
- Zhang, X.-J., Li, W., Ma, Q., Thorne, R. M., Angelopoulos, V., Bortnik, J., et al. (2016). Direct evidence for EMIC wave scattering of relativistic electrons in space: EMIC-Driven Electron Losses in Space. *Journal of Geophysical Research: Space Physics* 121, 6620–6631. <https://doi.org/10.1002/2016JA022521>
- Zhang, X.-J., Mourenas, D., Artemyev, A. V., Angelopoulos, V., & Thorne, R. M. (2017). Contemporaneous EMIC and whistler mode waves: Observations and consequences for MeV electron loss: SIMULTANEOUS EMIC AND WHISTLER OBSERVATIONS. *Geophysical Research Letters* 44, 8113–8121. <https://doi.org/10.1002/2017GL073886>
- Zhao, H., Baker, D. N., Li, X., Jaynes, A. N., & Kanekal, S. G. (2019). The Effects of Geomagnetic Storms and Solar Wind Conditions on the Ultrarelativistic Electron Flux Enhancements. *Journal of Geophysical Research: Space Physics* 124(3), 1948–1965. <https://doi.org/10.1029/2018JA026257>
- Zhao, H., Friedel, R. H. W., Chen, Y., Reeves, G. D., Baker, D. N., Li, X., et al. (2018). An Empirical Model of Radiation Belt Electron Pitch Angle Distributions Based On Van Allen Probes Measurements. *Journal of Geophysical Research: Space Physics* 123(5), 3493–3511. <https://doi.org/10.1029/2018JA025277>
- Zhao, H., & Li, X. (2013). Inward shift of outer radiation belt electrons as a function of Dst index and the influence of the solar wind on electron injections into the slot region. *Journal of Geophysical Research: Space Physics* 118, 756–764. <https://doi.org/10.1029/2012JA018179>